PHYSICAL REVIEW B VOLUME 25, NUMBER 11 1 JUNE 1982

Monte Carlo study of melting in two dimensions

Jan Tobochnik* and G. V. Chester
Laboratory of Atomic and Solid State Physics, Cornell University, Ithaca, New York 14853
(Received 9 February 1981; revised manuscript received 19 October 1981)

We present the results of Monte Carlo simulations of the two-dimensional Lennard-Jones system. The energy, pressure, structure factor, elastic constants, and $\langle u^2 \rangle$ have been computed at several temperatures along three isochores. In addition, we have studied the distribution of disclinations and dislocations on the same isochores. There is a well-defined solid phase and a well-defined fluid phase. The nature of the transition between these two phases cannot be unambiguously determined from our data. We are also unable to determine whether or not there is a hexatic phase. Somewhat more limited data are presented for the hard-disc system. The transition between the solid and liquid phases of the system appears to be first order.

I. INTRODUCTION

It is now well established[1-3] that a wide class of two-dimensional solids does not display the positional order that is characteristic of three-dimensional solids. The first theoretical discussions of this behavior were given by Peierls[4] and Landau.[5] A rigorous discussion, based on the Bogolyubov inequality, was provided by Mermin.[1] This theoretical work shows that if the particles are assumed to be localized near a set of lattice sites then their mean-square displacement from these sites will diverge like $\ln N$, and that the Fourier components of the density ρ_k will vanish exponentially fast. Here N is the number of particles in the system. The height of the "Bragg" peaks are weaker in two dimensions[6] behaving as $N^{1-\eta_G/2}$, where η_G is a number less than unity and depends on the square of the reciprocal-lattice vector. These results lead naturally to the question: How does one characterize a two-dimensional solid? Perhaps the most obvious way of characterizing such a solid is that it should possess a finite shear modulus.[7] If this feature is present, then we would naturally use the term "solid." A second characteristic of two-dimensional solids, which we will study in detail, is that they possess long-range orientational order. By this we mean that the orientation of particles in the local neighborhood of a point A is correlated with the orientation of those around a point B, no matter how distant B is from A. This remarkable property was first pointed out by Mermin[1] and first observed in simulation studies by Gann *et al.*[3]

Most of the computer simulations carried out prior to 1979 were concerned with establishing the equation of state, computing the structure function of the fluid phase and locating the melting transition. Simulations for both the hard-disc system[8] and the Lennard-Jones (LJ) system[9] showed that a melting transition was present. Alder and Wainwright[10] simulated what appeared to be two-phase coexistence. Young and Alder[2] showed convincing evidence that $\langle u^2 \rangle$, for hard discs, grows as $\ln N$ for N in the range $10-10^4$.

The description we have given of a two-dimensional solid leads immediately to the question: How does such a solid melt? Is it a first-order transition in which the long-range angular order abruptly disappears, or is it a transition of higher order? The theoretical framework in which this transition is usually discussed was developed by Kosterlitz and Thouless (KT).[11,12] They proposed a general mechanism for two-dimensional phase transitions, including the melting of two-dimensional solids. Their basic idea was that in two-dimensional systems, with continuous symmetry, topological defects will be thermally excited and will eventually destroy the order. Examples of such defects are spin vortices in magnetic systems, superfluid vortices in helium, and dislocations and disclinations in solids. We discuss these defects in more detail in the Appendix. For energetic reasons these excitations will be excited, at low temperatures, as bound pairs of opposite "sign." As the temperature is increased, the bound pairs will eventually start to break up and, at this point, the "order" of the low-temperature phase is destroyed and a phase transformation takes place to a less ordered phase. In this theory two-dimensional melting occurs when bound pairs of dislocations begin to break up into free dislocations. Computer simulations[13,14] have shown that the KT theory for the two-dimensional planar magnet is basically correct. There is good agreement between theory[15,16] and experiment[17] for thin helium films.

The purpose of this paper is to present the results of Monte Carlo simulations on the two-dimensional Lennard-Jones system over a wide range of density and temperature. We have supplemented this work with some smaller scale simulations of the hard-disc

system. These simulations were carried out to test the underlying ideas of Kosterlitz and Thouless and to see whether we could verify the more quantitative predictions of the theories of Halperin and Nelson (HN)[18] and Young.[19] These authors used renormalization-group techniques to make quantitative predictions based on the ideas of Kosterlitz and Thouless. We now summarize the results of this theory.

A. Phases of the system

The most striking prediction of the HN theory is that the melting process may take place in two steps. The solid first melts into a hexatic phase. Then the hexatic phase makes a transition into a disordered fluid. We shall describe the nature of the phases below. For the moment, we note that this two-step process is merely a possibility. It is not a universal prediction of the theory. A single-step process might replace it. In Fig. 1(a), we show a schematic phase diagram in which there is a bounded region of hexatic phase. At temperatures above T_a the transition is a single-step process; below T_a it is a two-step process. Two other examples of possible phase diagrams are shown in Figs. 1(b) and 1(c). In Fig. 1(b) there is an unbounded "strip" of hexatic phase, and melting is always a two-step process. In Fig. 1(c) there is no region of hexatic phase; here melting is always a single-step process.

According to Kosterlitz and Thouless the melting transition is the point where dislocation pairs begin to unbind. If at that point the disclinations which make up a dislocation remain bound, then we expect a hexatic phase just above the melting point. When the disclinations unbind, the hexatic order is destroyed and we have a normal fluid.

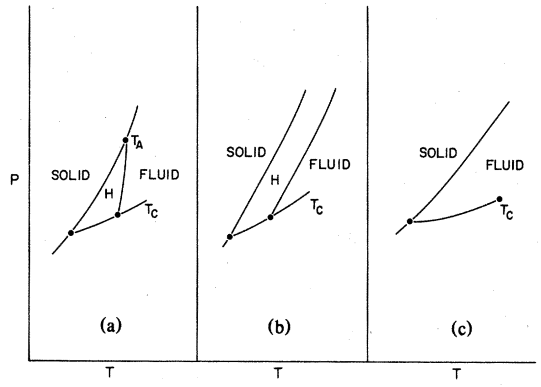

FIG. 1. These figures [(a), (b), and (c)] show the three possible types of phase diagram for melting in two dimensions. (a) shows a bounded region of hexatic phase H; (b) an unbounded region of hexatic phase H; and in (c) there is no region of hexatic phase.

B. Solid phase

(i) In this phase there are long-range angular correlations but no long-range positional correlations. At very low temperatures, where only bound pairs of dislocations are excited, the angular correlations can be computed from harmonic theory. The angular correlation function is defined by the equation

$$g_6(r) = \langle \exp\{i6[\theta(r) - \theta(0)]\} \rangle \ . \tag{1.1}$$

Here θ is the angle between a vector joining two nearest neighbors and some fixed direction, and r is the distance between two sets of nearest-neighbor pairs. The factor 6 naturally arises from the sixfold symmetry in a triangular lattice. Our definition differs from that of Ref. 25, where $g_6(r) \equiv \langle \psi(r)\psi(0) \rangle$ and $\psi(r) = \sum_{i=1}^{6} e^{i6\theta(r)}$ is an average over all bonds connecting an atom located at position r. We do not perform this average and our values of r are located at the midpoints of the bonds. The result is that we do not find the large oscillations in $g_6(r)$ reported in Ref. 25. The long-range orientational order manifests itself through the long-range behavior of $g_6(r)$: $g_6(r)$ tends to a constant as r increases indefinitely.

At higher temperatures in the solid phase $g_6(r)$ still shows long-range order but its asymptotic value is now reduced by both anharmonic motions and by the excitation of bounds pairs of dislocations.

(ii) As we have already mentioned, we expect to see thermally excited bound pairs of dislocations, increasing in number as we approach the melting point. Just before melting we should see some of these pairs unbind. This is predicted to be the signal for the onset of melting.

(iii) Near melting there is a universal behavior of a combination of the two Lamé constants λ and μ.[20] The quantity $K = 4\mu(\mu+\lambda)/(2\mu+\lambda)$ is predicted to be given by

$$K^{-1} = (1/16\pi)(1 - c|t|^{\nu}) \ . \tag{1.2}$$

Here $t = (T - T_m)/T_m$, where T_m is the melting temperature, ν is an index with the universal value of 0.369, and c is a constant. The Lamé coefficients λ and μ are in units of $k_B T/a_0^2$. The melting temperature is defined as the point at which K drops suddenly from a universal value of 16π to 0. These predictions for K are universal in the sense that they should hold at all points on and near the melting curve as long as the transformations are controlled by the KT mechanism. Systems with different potentials will show this universal behavior—again provided that the melting mechanism is that suggested by KT.

(iv) We conclude by mentioning the predictions for the peaks in the structure factor $S(k)$. These predictions are based on harmonic theory[6] and can be viewed as being independent of KT theory. For

small q near a reciprocal-lattice vector $\vec{G}$,

$$S(|\vec{G}-\vec{q}|) \sim q^{-2+\eta_G} \quad . \tag{1.3}$$

At a reciprocal-lattice vector,

$$S(G) \sim 4N^{1-\eta_G/2} \quad . \tag{1.4}$$

Here N is the number of particles in the system and

$$\eta_G = G^2(3\mu+\lambda)/4\pi\mu(2\mu+\lambda) \quad . \tag{1.5}$$

Equation (1.3) tells us the shape of the "Bragg" peak and Eq. (1.4) tells us the height of these peaks. The exponent η_G is a number less than unity.[6]

C. Hexatic phase

We have already mentioned that there are at least two possibilities suggested for how melting takes place. Either the solid melts into a hexatic phase or into a disordered fluid. The hexatic phase is in many ways "fluidlike."

It is characterized as follows:

(i) The angular correlations, as defined previously, decay slowly,

$$g_6(r) \sim r^{-\eta_6} \quad ,$$

where η_6 is always less than $\frac{1}{4}$. In this phase there are no infinite range angular correlations.

(ii) The hexatic phase possesses a finite Frank constant K_A.[18,21] The Frank constant is a measure of the resistance of the hexatic phase to local angular distortions. This constant is related to the exponent η_6 by the equation

$$K_A = \frac{18k_BT}{\pi\eta_6} \quad .$$

The Frank constant is expected to diverge as the solid phase is approached from the high-temperature side. It has a universal jump of $72/\pi$ at the temperature where the hexatic order disappears and normal fluid order takes over.

D. Fluid phase

This is a normal fluid phase with exponentially decaying angular correlations and a vanishing Frank constant.

We should conclude this description on the HN theory by emphasizing the two basic assumptions on which it is built. First, that the unbinding of pairs of topological defects is the mechanism by which the two-dimensional order is destroyed. If other mechanisms are more important, then the topological defects may not control the melting transition. For example, the order might be destroyed by the creation of significant numbers of point defects. Second, it is assumed that the density of dislocation pairs is sufficiently low so that the pairs can be treated as a dilute system. Both of these assumptions can be investigated by means of computer simulation.

E. Recent computer simulations

We now summarize the results of the recent computer simulations. This summary will lead us naturally to the most controversial question concerning two-dimensional melting: Is melting a first-order transition or of the type suggested by KT? Two simulation studies have recently been reported which support the idea that melting in two dimensions is first order.

Abraham,[22] working with a constant pressure ensemble, has found strong hysteresis effects in the Lennard-Jones system. Hysteresis is a natural phenomenon if the transition is first order. It could also occur if the simulated system were for some reason showing strong metastability. Toxvaerd[23] has published pictures, derived from molecular dynamics simulations on the Lennard-Jones system, which appear to show two-phase equilibrium between a solid and a fluid just above the melting temperature. The diagrams show clear regions of ordered phase and regions of disordered fluidlike phase. They are very similar to the picture published much earlier by Alder and Wainwright.[10] While these results are, at first sight, quite convincing, we shall see that their interpretation is not unambiguous.

Two other recent studies have produced results that support the predictions of the Halperin-Nelson theory. Morf[7] has published results for the two-dimensional Coulomb system which show that the elastic constant K obeys the predictions of HN theory.[24] There is a discontinuity in K of approximately equal to 16π and its temperature dependence just below the discontinuity temperature is close to that given by Eq. (1.2). These results strongly support the idea that the melting transition is well described by the theory. The published data throw no light on the existence of the hexatic phase. The molecular dynamics study carried out by Frenkel and McTague[25] does suggest that the Lennard-Jones system will have a hexatic phase for some temperatures and pressures. These authors find a region in which the angular correlations, defined by Eq. (1.7), decay slowly across the system. This is, of course, a characteristic feature of this phase. Again, we shall see that the interpretation of these data is also not unambiguous.

In Sec. II we describe our results for two low-density isochores ($\rho^*=0.856$ and $\rho^*=0.888$). Here $\rho^*=\rho\sigma^2$, with ρ the areal density and σ the LJ length parameter. The cutoff in the LJ potential was

3σ. We give results for the order in the solid phase, the elastic constants and the structure factor.

The angular correlations were studied at several temperatures along these isotherms. We shall see that it is difficult to give an unambiguous interpretation of their behavior. In addition, we have, using the Voronoi[26] polygon construction, counted both disclinations and dislocations in the solid phase and above the melting point. These data allow us to both compute the "core" energy of a bound pair of dislocations and to qualitatively test the underlying hypotheses of KT theory. In Sec. III we give a similar set of data for a high-density isochore $\rho^* = 1.143$ of the Lennard-Jones system. At this density, both the thermodynamic functions and the elastic constants show strikingly different behavior. Section IV is devoted to a similar presentation of the data for the hard-disc system. The behavior of this system is very similar to that of the high-density Lennard-Jones system. A very striking feature is that it, too contains bound pairs of dislocations at low temperatures.

In Sec. V we give a discussion of our results. We are able to convincingly demonstrate that the solid phases behave as expected and that there is a definite melting transition. We are not, however, able to show convincingly whether or not a hexatic phase exists and whether or not the melting transition is first order. There is indeed a fundamental ambiguity which plagues the interpretation of nearly all the data in the region above melting. A two-phase region can, it turns out, readily mimic the behavior of a hexatic phase. We are, at this time, unable to demonstrate a clear distinction between them.

We conclude our discussion by suggesting several simulation studies that might illuminate, and even eliminate, some of the present confusion.

The Appendix contains a discussion of dislocations, disclinations, and Voronoi polygons.

II. LOW-DENSITY LENNARD-JONES SYSTEM

In this section we will present our results for the low-density Lennard-Jones system. Our simulations were carried out on the two isochores $\rho^* = 0.856$ and $\rho^* = 0.888$. For comparison we recall that the two-dimensional (2D) triple-point reduced density is estimated[27] to be 0.815. On each of these isochores we made successive Monte Carlo runs increasing and decreasing the temperature. At several temperatures we collected very extensive data. In Table I we show

TABLE I. Simulation results for the isochore $\rho^* = 0.856$. T^*, E^*, and P^* are the reduced temperature, energy, and pressure, respectively. K is the elastic constant $4\mu(\mu+\lambda)/(2\mu+\lambda)$. The column labeled "$N$ pass" gives the number of Monte Carlo passes made at that temperature.

T^*	E^*	P^*	K	N pass
0.500	−2.7440	0.977	82.0	3900
0.550	−2.7071	1.320	68.1	2560
0.630	−2.6503	1.838	67.3	10240
0.640	−2.6409	1.924	64.6	5120
0.650	−2.6341	1.988	61.2	5120
0.660	−2.6290	2.033	61.4	10240
0.670	−2.6190	2.121	59.0	20480
0.680	−2.5939	2.403	54.0	10240
0.685	−2.5636	2.652	31.0	5120
0.690	−2.5876	2.380		15360
0.700	−2.5481	2.808		15360
0.710	−2.5560	2.724		15360
0.720	−2.5458	2.915		5120
0.725	−2.5449	2.825		5120
0.730	−2.5249	3.006		5120
0.740	−2.4997	3.213		5120
0.760	−2.4662	3.493		5120
0.770	−2.4503	3.636		5120
0.790	−2.4372	3.747		5120
0.810	−2.4099	3.962		5120
0.830	−2.3896	4.133		5120
0.860	−2.3830	4.536		5120
0.875	−2.3531	4.446		5120

some of the data for the isochore $\rho^*=0.856$; the last column gives the total number of Monte Carlo passes made at each temperature. Table II provides the same summary for $\rho^*=0.888$. At nearly all temperatures several Monte Carlo runs were made from different starting configurations. ($T^* \equiv k_B T/\epsilon$ where ϵ is the LJ strength parameter.)

Our data clearly show that along both of these isochores there are three distinct regions. At low temperatures there is a solid phase, at high temperatures there is a normal fluid phase, and at intermediate temperatures there is a complex region. This region may tentatively be identified with a hexatic phase or with a two-phase region. As we present our data, we will carefully weigh the evidence for and against each interpretation.

TABLE II. Simulation results for the isochore $\rho^*=0.888$. T^*, E^*, and P^* are the reduced temperature, energy, and pressure, respectively. K is the elastic constant $4\mu(\mu+\lambda)/(2\mu+\lambda)$. The column labeled "$N$ pass" gives the number of Monte Carlo passes made at that temperature.

T^*	E^*	P^*	K	N pass
0.5000	−2.8415	1.9041	118.7	6400
0.7500	−2.6483	3.6350	87.9	10 000
0.8000	−2.6064	4.0022	83.6	8000
0.9000	−2.5344	4.6442	74.7	13 600
1.0000	−2.4435	5.2747	63.0	40 800
1.0250	−2.4297	5.4733	64.1	20 000
1.0500	−2.3863	5.9213	57.0	44 800
1.0600	−2.3850	5.8266	54.2	12 800
1.0650	−2.3141	6.5102	16.5	12 800
1.0700	−2.3154	6.4987		6400
1.0750	−2.3032	6.6072		35 200
1.0800	−2.3143	6.5298		6400
1.0850	−2.3188	6.4836		12 800
1.0900	−2.3105	6.4917		6400
1.0950	−2.3098	6.4594		6400
1.1000	−2.2346	7.1476		21 600
1.1100	−2.2525	7.0079		92 000
1.1200	−2.2059	7.3820		25 600
1.1400	−2.2036	7.3982		12 800
1.1500	−2.1771	7.6187		9600
1.1600	−2.1548	7.7896		25 600
1.1700	−2.1553	7.7931		16 800
1.1800	−2.1692	7.6995		12 800
1.1900	−2.1478	7.8658		6400
1.2000	−2.1349	7.9686		44 000
1.2200	−2.0975	8.2526		6400
1.2500	−2.0833	8.3866		6400
1.2700	−2.0491	8.6441		16 000
1.3000	−2.0522	8.6545		6400
1.3200	−2.0204	8.9258		6400
1.3500	−2.0007	9.0690		6400
1.3700	−1.9666	9.3207		6400
1.4000	−1.9464	9.4905		19 200
1.5000	−1.8804	10.0355		13 800
1.6000	−1.7888	10.7826		6600

A. Energy and pressure

The energy and pressure are the two thermodynamic quantities we derived from our simulation data. Other thermodynamic quantities, such as the specific heat and free energy, can be computed from these quantities by differentiation or integration.

The reduced energy ($E^* = E/\epsilon$) is shown as a function of the reduced temperature $t = (T - T_m)/T_m$ in Fig. 2. We have chosen this reduced temperature with T_m the temperature at which the elastic constant K drops suddenly to zero (see Sec. II D). Tables I and II show the data for these densities. The uncertainty in the data is shown by the scatter in the points. At both densities there is a pronounced change in the shape of the curves at $t = 0$. This implies a rapid increase in the specific heat at the same temperature as the elastic constant K drops to zero. There is, however, another change in the slope of these curves at a somewhat higher temperature. This is clear from Fig. 2. For $\rho^* = 0.856$ the second anomaly occurs at $1.13T_m$, while for $\rho^* = 0.888$ the anomaly occurs at $1.06T_m$. The precise position of these anomalies is difficult to locate. They are considerably weaker than those at lower temperatures. The presence of these two anomalies on each isochore implies that the specific heat will have a fairly sharp maximum just above T_m. The standard analysis of the KT transition[18] leads to broad peak in the specific heat above the transition temperature. This disagreement with the theory may be explained by the fact that the density of defect pairs is rather large just below T_m. The pairs also show a strong tendency to cluster. These points will be discussed in more detail in Sec. II G. We note that the behavior of the specific heat in the two-dimensional Lennard-Jones system is somewhat similar to that found in the planar spin system.[13,14] In that system, also, strong clustering of defect pairs was observed.

The sharp rise in the energy, and hence specific heat, as a function of temperature is in qualitative agreement with a KT transition. It is also in qualitative agreement with a first-order transition. If the melting transition is first order, then the region between the two "kinks" in the energy curves could be interpreted as the two-phase region. As one passes through T_m a small amount of liquid phase appears, causing a change in the shape of the energy curve. At a higher temperature the last piece of solid phase disappears and the energy curve again shows an anomaly. Thus the temperatures at which we observe the sudden changes in slope mark the boundaries of the two-phase region; the lower temperature corresponds to melting at constant density, the upper temperature to freezing at constant density. This interpretation can be compared with the data from Toxvaerd's[23] simulation study of freezing and melting. From this comparison we find that his two-phase region is about 30% wide in temperature, whereas our widths are 13% and 4% wide, respectively, on the two isochores. While the discrepancy between 30% and 13% might be removed by im-

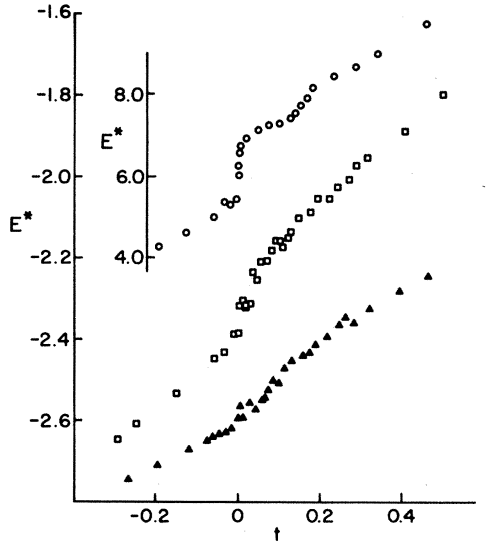

FIG. 2. Reduced energy $E^* = E/\epsilon$ as a function of reduced temperature $t = (T^* - T_m^*)/T_m^*$. Here T_m^* is the temperature at which the elastic constant K drops to zero: ○ corresponds to $\rho^* = 1.143$, □ corresponds to $\rho^* = 0.888$, and ▲ to $\rho^* = 0.856$. Note that the energy scale has been changed for $\rho^* = 1.146$.

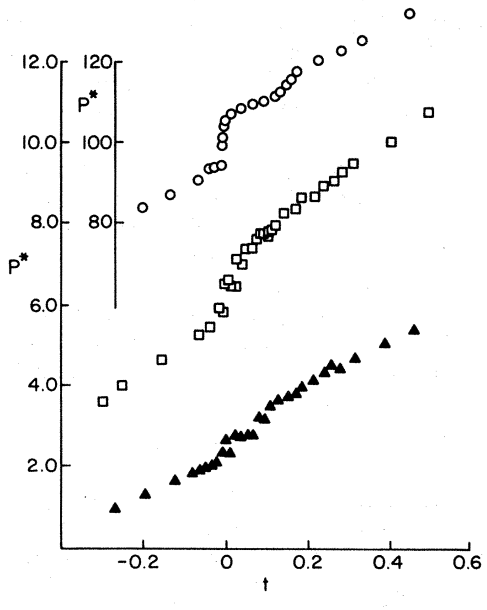

FIG. 3. Reduced pressure $P^* = P\sigma^2/\epsilon$ as a function of reduced temperature $t = (T^* - T_m^*)/T_m^*$. The notation on the three curves is the same as in Fig. 2.

proved simulations, the discrepancy between 4% and 30% is outside the range of our errors. We thus have a puzzle. Our data are roughly consistent with a two-phase interpretation but are not in agreement quantitatively. There is, however, the possibility that our simulations may not have reached true equilibrium and that we are looking at the boundaries of metastable regions. We shall discuss this suggestion in detail in Sec. V.

The pressure behaves in the same way as the energy. The data are shown in Fig. 3. There are no predictions of the behavior of P as a function of temperature from the KT theory. However, there is no reason to believe that our data are inconsistent with the theory. If the transitions were first order than the region between the two changes in slope arises because a constant density system will follow the melting curve in the P-T plane until the density of the liquid phase equals that of the solid.

We shall see that the data we have obtained on the high-density Lennard-Jones system may throw some light on the situation at low densities. These data will be discussed in Sec. III.

B. Displacement of the particles

We computed the mean-square displacement $\langle u^2 \rangle$ of the particles from their lattice sites for all temperatures in the solid phase and for a few temperatures just above T_m. For a large finite system we expect $\langle u^2 \rangle$ to behave like $\ln N$, where N is the number of particles. This prediction has been verified in the hard-disc[2] and the one-component plasma system.[3] We found that in our 1024-particle system and for $\rho^* = 0.888$, $\langle u^2 \rangle$, in units of σ^2, increased from 0.023 at $T^* = 0.50$ to 0.25 at $T^* = 1.05$. For this density $T_m^* = 1.06$. At T_m^*, $\langle u^2 \rangle$ rose abruptly, showing that some of the particles were becoming delocalized. Harmonic theory predicts that $\langle u^2 \rangle$ is proportioned to the temperature. We found this to be true for temperatures up to $T^* = 0.90$. Between this temperature and T_m^*, $\langle u^2 \rangle$ increased faster than the first power of the temperature.

The values $\langle u^2 \rangle$ provide us with direct evidence that in the solid phase the particles are well localized and that at T_m^* the particles start to diffuse freely.

C. Structure function

In the low-temperature solid phase, harmonic theory[6] should provide a reasonable guide to the behavior of the structure function $S(k)$. In the Introduction we summarized the two main predictions, Eqs. (1.3) and (1.4). In Fig. 4 we show our data for $S(|G-q|)$ for small $|\vec{q}|$ and three different reciprocal-lattice vectors $\vec{G}$. For each temperature and reciprocal-lattice vector the slope of the curves of $\ln S$

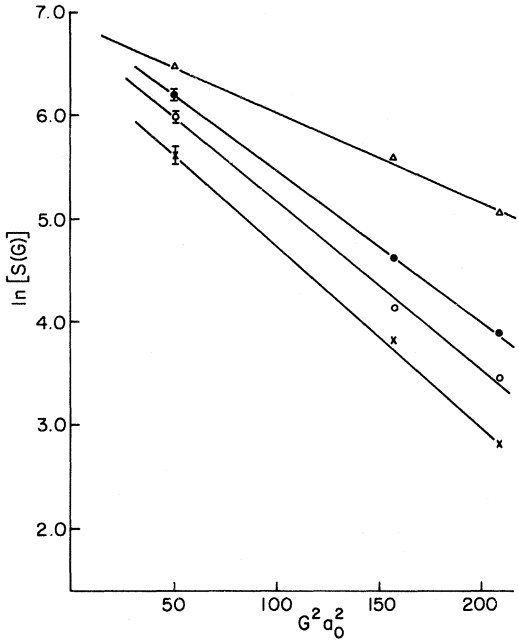

FIG. 4. $\ln S(\vec{G})$ vs $G^2 a_0^2$, where $\vec{G}$ is a reciprocal-lattice vector, a_0 the lattice spacing, and $S(\vec{G})$ the static structure factor. The density $\rho^* = 0.888$. The curves from the top down correspond to reduced temperatures $T^* \equiv k_B T/\epsilon$ equal to 0.5, 0.75, 1.025, and 1.06, respectively. Theory predicts that the *slope* of these curves is equal to $0.51 \ln 4N(\eta_G/G^2)$. The exponent η_G is defined in the text and N is the number of particles in the system.

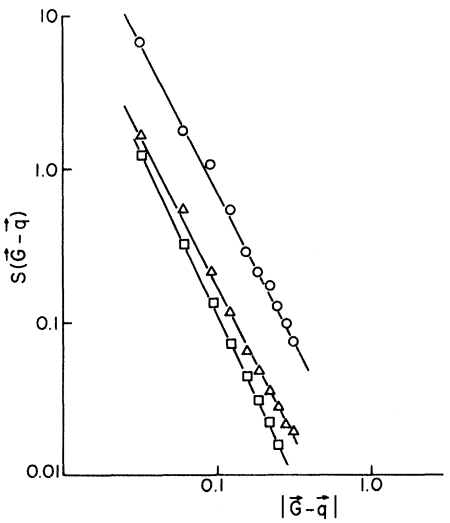

FIG. 5. Structure factor $S(|\vec{G}-q|)$ for q near a reciprocal-lattice vector. The vectors $\vec{G}$ and $\vec{q}$ are in units σ^{-1}. The three curves correspond to different temperatures, densities, and reciprocal-lattice vectors. □ is for $T^* = 0.5$, $\rho^* = 0.888$, and $G = (2\pi/a_0, 2\pi/\sqrt{3}a_0)$; Δ is for $T^* = 0.63$, $\rho^* = 0.856$ and $G = (2\pi/a_0, 2\pi/\sqrt{3}a_0)$; ○ is for $T^* = 7.2$, $\rho^* = 1.143$ and $G = (0, 4\pi/\sqrt{3}a_0)$.

TABLE III. The exponent η_G, see Eq. (1.5) for three densities. The third column gives η_G calculated from the height of the structure factor at various reciprocal-lattice vectors. The fourth column gives η_G computed directly from the elastic constants. The two sets of values are all consistent with each other within the statistical errors which are about 10% for each method of computation.

T^*	ρ^*	η_G ($\times 10^{-3}$) from $S(G)$	η_G ($\times 10^{-3}$) from $\mu+\lambda$	% diff
0.63	0.856	3.4	4.1	+19.0
0.64		3.9	4.2	+7.0
0.65		3.6	4.3	+18.0
0.66		4.0	4.4	+10.0
0.67		4.1	4.6	+11.0
0.5	0.888	2.0	2.3	+14.0
0.75		3.4	3.1	−9.0
0.8		3.5	3.2	−9.0
0.9		3.5	3.8	+8.0
1.025		3.7	4.2	+13.0
1.05		5.7	4.8	−17.0
1.06		4.3	5.3	+21.0
7.0	1.143	4.1	3.5	−16.0
7.2		4.6	3.7	−22.0
7.3		4.5	3.8	−17.0
7.4		4.2	3.6	+7.0

vs q is so close to -2 that we cannot extract a reliable value of η_G from the data. This behavior is completely different from the behavior in three dimensions when $S(|G-q|)$ diverges as a delta function for small q. Figure 5 shows plots of $\ln S(G)$ vs G^2. The data are sufficiently accurate that we can now extract a value of η_G with an accuracy of about 10%. These values are given in Table III. They allow us to make an important consistency test. From η_G, obtained from $S(|G|)$, we can easily compute values of the quantity $(3\mu+\lambda)/4\pi\mu(2\mu+\lambda)$ [see Eq. (1.5)]. We can also compute μ and λ directly[28] and hence obtain values of this quantity in an independent manner. In Sec. III we will compare the values obtained by these two methods.

At the melting temperature the peaks in the structure function drop dramatically in value. In the solid phase, just below T_m^*, the value of $S(G)$ for the smallest reciprocal-lattice vector is about 300. Just above T_m the value fluctuates about a mean which is approximately ten times smaller. Thus S gives a clear signal that the system has melted.

Throughout the intermediate region the structure function fluctuates strongly. It takes on values ranging from unity to 100. The mean values computed over long Monte Carlo runs are in the range 30–50. These fluctuations suggest that in this region there is some spatial order which is fluctuating on long Monte Carlo time scales. It does not seem possible to use $S(k)$ values to distinguish between a hexatic phase and a two-phase region.

In the disordered fluid phase we find values of $S(k)$ typical of an isotropic two-dimensional fluid.[3,9]

D. Elastic constants

The elastic constants of the solid phase can be computed directly from the expressions given by Squire *et al.*[28] There are two independent Lamé coefficients λ and μ.[20] For a triangular lattice these can be related to C_{11} and C_{22}:

$$C_{11}=C_{22}=2\mu+\lambda \ . \tag{2.1}$$

The expressions for the elastic constants contain differences between fairly large quantities. Our data at low temperatures show quite large fluctuations leading to statistical errors of about 10%. There are two consistency checks we can apply to our data. The simplest is to see whether the equality (2.1) is satisfied. We find that it is satisfied within our errors. The second is to compute the exponent η_G from the elastic constants [Eq. (1.5)] and compare this value with that obtained from a direct simulation of the

structure function (see Sec. II C). Again we find consistency within the statistical fluctuations of our data. These two tests give us confidence that we are computing the elastic constants with reasonable accuracy (see Table III).

We now turn to a discussion of a key quantity in the HN theory, the elastic constant K. This is defined in Eq. (1.2). If the melting transition is mediated by the unbinding of dislocation pairs then K should have the universal temperature dependence give by Eq. (1.2), and this implies a universal discontinuity of 16π at melting. The elastic constant K is mainly determined by μ and is comparatively insensitive to λ. This is fortunate because μ shows fluctuations of about 10%, but those in λ are much larger. The uncertainty in K is only a few percent when T is much less than T_m and about 15% near T_m. In Fig. 6 we show plots of K against reduced temperature. The curves are fits to the data within 10% of T_m^* of the form suggested by theory [Eq. (1.2)]. As can be seen, the fits[29] are quite good. The best values for the parameters in Eq. (1.2) are at $\rho^*=0.856$, $T_m^*=0.682$, $\nu=0.38$, and $C=0.65$, while at $\rho^*=0.888$, $T_m^*=1.061$, $\nu=0.28$, and $C=0.45$. In each case the deviation of the fit from the data is of order unity. If we fix T_m^*, then at $\rho^*=0.856$, ν changes to 0.31 for $T_m^*=0.681$ and to 0.43 for $T_m^*=0.683$. Thus our data strongly point to ν being less than 0.5 and our two best values of ν are very close to the theoretical value of 0.369. The data show an extremely rapid drop in K. Since the data have been shown to fit the theoretical predictions very well, the magnitude of the discontinuity in K is also confirmed. The points on the curve at $t=0$ represent fluctuations in K as we cool the system through the melting point. We plan to carry out further simulations to clarify this behavior. We conclude that the low-density Lennard-Jones system agrees with the melting prediction of the HN theory very well indeed. The behavior at high densities is very different and will be discussed in Sec. III.

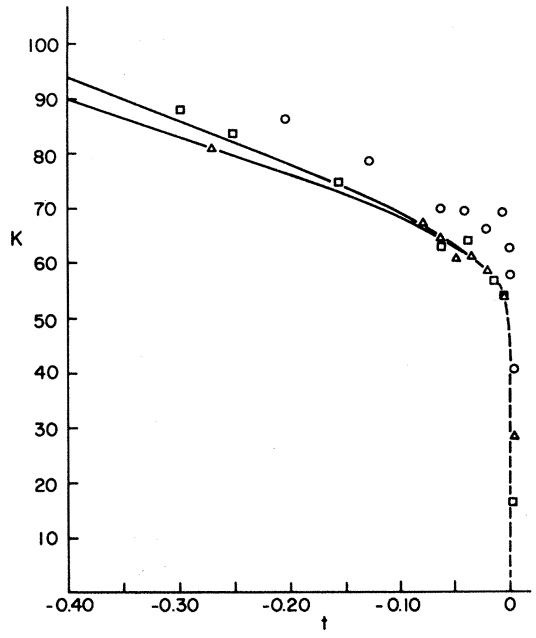

FIG. 6. Elastic constant $K=4\mu(\mu+\lambda)/(2\mu+\lambda)$ vs the reduced temperature $t=(T^*-T_m^*)/T_m^*$. The points marked with ○ are for a density $\rho^*=1.143$; those marked with □ are for $\rho^*=0.888$; and those marked Δ are for $\rho^*=0.856$. The two lower curves are least-square fits to the data points from $t=0.20$ to just below $t=0$.

At a first-order phase transformation we also expect a discontinuity in the elastic constants. However, there is no reason to believe that the discontinuity will have a universal value or that the temperature dependence just below T_m will be universal. The universal behavior of K is a unique prediction of the HN theory. As long as an elastic continuum description of dislocations and dislocation pairs is adequate, then one can show that the solid will be unstable to the creation of free dislocations if K is less than 16π. Our data confirm this instability. We conclude that the melting transition, at low densities, is described very well by the HN theory. It is, of course, possible that we have superheated the solid and that we are watching the collapse of a metastable system.[30] We defer further discussion of this suggestion to Sec. V.

E. Angular correlation function

In the hexatic phase of the HN theory, the angular correlation function, defined by Eq. (1.1), shows a slow-power law decay towards zero:

$$g_6(r) \sim r^{-\eta_6}$$

for large r. Here η_6 is a temperature-dependent exponent whose value is predicted to be always less than $\frac{1}{4}$. In the hexatic phase there is thus a remnant of orientational order. This is to be contrasted with the behavior of $g_6(r)$ in the solid phase, where it tends asymptotically to a constant. In a normal fluid phase the angular correlations decay exponentially to zero. An example of $g_6(r)$ is shown in Fig. 7.

On both isochores and for all temperatures below the melting temperature we find that $g_6(r)$ tends asymptotically to a constant. For example, just below T_m^*, the asymptotic value is approximately 0.35. Perfect correlation would be 1.0. In the solid phase the asymptotic values fluctuate by 1% to 3% during a run of several thousand passes. The solid at these densities and temperatures clearly exhibits long-range orientational order.

At temperatures much greater than T_m^*, $g_6(r)$ de-

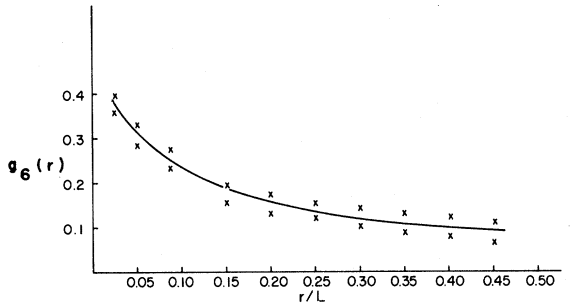

FIG. 7. Angular correlation function $g_6(r)$ as a function of distance. Here L is the length of the side of the box containing the particles. The solid curve represents the general trend of the data over very long Monte Carlo runs. The data showed very long-term fluctuations. The ×'s show the range of these long-term fluctuations. The curve can be represented by $r^{-\eta}$ with $\eta \simeq 0.3$.

cays very rapidly to zero. There is clearly a high-temperature fluid phase in which the angular correlations are rapidly damped out. This occurs at temperatures above $1.4T_m^*$. We made successive Monte Carlo runs, gradually lowering the temperature, and monitored the behavior of $g_6(r)$. Qualitatively, we found a rapid increase in the range of the correlations. However, large fluctuations in the orientational order were present. We analyzed our data by assuming an exponential form for the correlation function

$$g_6(r) \sim \exp(-r/\xi_6) \ ,$$

and we assumed that ξ_6 was given by

$$\xi_6 \sim \exp(bt_2^{-1/2}) \ .$$

This is the form suggested by KT theory. Here b is a constant and $t_2 = (T^* - T_2^*)/T_2^*$. Thus ξ_6 is expected to diverge at some unknown temperature T_2^*. Much of our data could be reasonably well fitted by these forms for $g_6(r)$ and $\xi_6(t)$. There were, however, large fluctuations in $g_6(r)$ which made the determination of ξ_6 very difficult. Our best fits suggest that ξ_6 does diverge: we estimate that, for $\rho^* = 0.888$, $T_2^* = 1.26$, while for $\rho^* = 0.856$, $T_2^* = 0.82$. Both of these values of T_2^* are significantly higher than the values of T_m^*. It is this fact which suggests to us that there is a clearly defined intermediate region between T_m^* and T_2^*.

For temperatures just above T_m^*, $g_6(r)$ appears to decay very slowly across the system and appears to fit a power law. At somewhat higher temperatures the decay is more rapid, but still appears to fit a power law. In all of our simulation runs we found very large fluctuations over very long Monte Carlo "time" scales. Our data on $g_6(r)$, between T_m^* and T_2^*, can be fitted by a power law $g_6 \sim r^{-\eta_6}$. However, the fluctuations in the data produce the large uncertainties in the value of η_6. At $T^* = 1.11$, which is 5% above T_m^*, on the isochore $\rho^* = 0.888$, we ran a total of 75 000 passes and found $\eta_6 = 0.3 \pm 0.2$ (see Fig. 7). At higher temperatures η_6 is larger and so are the uncertainties in it. At $T^* = 1.11$ it took about 30 000 passes for η_6 to pass from its highest to lowest value. It is for this reason that we doubt that we have obtained equilibrium values for $g_6(r)$.

According to the HN theory, η_6 cannot exceed $\frac{1}{4}$ in the hexatic phase. This is actually a rather more general result; η_6 cannot exceed $\frac{1}{4}$ as long as the disclinations can be described by a macroscopic elastic theory. When the exponent exceeds $\frac{1}{4}$ the phase becomes unstable with respect to free disclinations and transforms into a disordered fluid. Since most of our values for η_6 are larger than $\frac{1}{4}$ there is a serious problem with the HN interpretation that the intermediate region is a hexatic phase. Either the disclinations cannot be described by a macroscopic elastic theory, or the intermediate region is not a hexatic phase. Two difficulties with our simulation should be pointed out. First, our system of 1024 particles may not be large enough for us to have reached the asymptotic region of $g_6(r)$. A simulation on a system of at least twice the linear size would be useful to test this hypothesis. Second, the very long time scale fluctuations lead to large uncertainties in the results of our analysis. We estimate that we would need to extend our runs by a factor of 10, at least, to remove the major part of this uncertainty.

It seems plausible that a two-phase region could also lead to a very slow decay of $g_6(r)$. In such a region the patches of solid will produce angular correlations which decay towards constant values, while the fluid regions will have correlations that decay rapidly to zero. An average of these two kinds of behavior taken with appropriate weights for the solid and fluid regions might well produce a power-law decay. The evidence we have found for a power-law decay is not adequate to distinguish between a hexatic phase and a two-phase region. If simulation on a larger system or with larger runs could more convincingly demonstrate a power law and produce precise values of η_6 close to those predicted by theory, then such a distinction might be made.

We end with some comments on how our data might be interpreted if the melting transition is first order. If the transition is first order, then T_2^* might be the temperature where the two-phase region ends. This gives a two-phase region which has a width in temperature of 20% of T_m^*. This is smaller than the width suggested by Toxvaerd, although we should again point out that we may be looking at the boundaries of metastable regions. If T_2^* is the beginning of the two-phase region, then near that temperature we

would expect $g_6(r)$ to gradually increase—as more and more solid forms. We see no evidence for this behavior, rather we tend to see a very rapid rise in g_6. Unfortunately, this behavior is beset with uncertainties induced by large fluctuations and no definite conclusion can be drawn.

F. Topological defects

The phase transitions in the HN theory of melting are caused by the unbinding of topological defect pairs. First, dislocation pairs unbind and then, at a higher temperature, the disclination pairs unbind. A dislocation in a triangular lattice can be regarded as a pair of disclinations of opposite disclinicity tightly bound together. We discuss these matters in detail in Appendix A. Thus it is important to determine if these defects are indeed important in the melting process.

The disclinicity enclosed by any closed circuit in the lattice can be determined by computing the change in the bond angle θ, modulo $\pi/3$, as the loop is traversed. If the disclinicity is zero then the change in θ will be zero. Otherwise the change in θ will be an integral multiple of $\pi/3$. If we have tightly bound pairs of disclinations then we must compute the disclinicity around a loop whose radius is of the order of a lattice spacing. To do this we must have a precise definition of the bond angles and thus of the nearest neighbors.[31] Such a definition is given by the Voronoi polygon construction explained in Appendix A. Once this construction is made, we can carry out the above procedure for the bond angles associated with each particle.

However, we show in the Appendix that all that is necessary is to count the vertices of the Voronoi polygon associated with each particle. A disclination of unit positive strength is located at a particle with five vertices (near neighbors) in its Voronoi polygon. One with unit negative strength has seven vertices (neighbors). Disclination of higher strengths are possible. In our simulations we found only one other kind, namely, of strength -2.

In the cold solid we find that there are only a small number of tightly bound disclinations. In Fig. 8 we show the positions of disclinations for a single configurations in a solid with $T^*=1.05$ and $\rho^*=0.888$. This is 1% below the melting temperature. Notice that even at this temperature the disclinations nearly all occur in quadruples. Such a quadruple corresponds to a bound pair of dislocations. In a periodic system such as ours the net disclinicity and the total Burgers vector must be zero. This is verified in all our simulations. Note also that there are some clusters of six disclinations. The Burgers vectors for a dislocation is perpendicular to the vector joining the two disclinations comprising the dislocation. We find

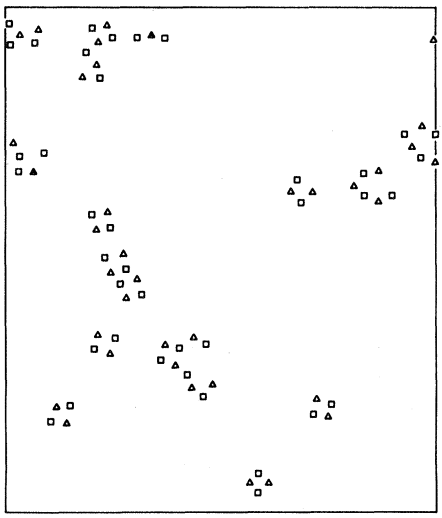

FIG. 8. Distribution of disclinations at $T^*=1.05$, $\rho^*=0.888$. A □ denotes a disclination of unit positive strength, i.e., a particle with five near neighbors; a Δ denotes a disclination of unit negative strength, i.e., a particle with seven near neighbors; and a ▲ a disclination of strength -2 with eight near neighbors. A closely bound pair $(+-)$ of disclinations is equivalent to a dislocation. The distribution corresponds, fairly closely, to a set of bound dislocation pairs. The temperature is just below the melting temperature for this density.

that these clusters of six disclinations still have a net zero Burgers vector. We also have a small number of disclinations of strength -2. These are located at particles with eight nearest neighbors. These disclinations always appear close to two others of strength $+1$.

Two disclination plots for $T^*=1.11$ and $\rho^*=0.888$ are shown in Figs. 9 and 10. This temperature is 5% above melting. The density of disclinations is quite different in the two pictures; large fluctuations are possible in the intermediate region between the disordered liquid and solid. The areas where no disclinations are found correspond to regions which appear well ordered on a plot of particle trajectories. Some free dislocations (pairs of disclinations not bound to other pairs) can be seen. This supports the contention of HN theory that melting is due to the unbinding of dislocation pairs. In Fig. 8 there are some disclinations which are more than two lattice spacings away from any other disclination. These could be free disclinations or they could be weakly bound. According to the HN theory, free disclinations should not appear until one is close to the second phase transition. Our analysis of the correlations of angular order suggests that this occurs at $T^*=1.26$.

At $T^*=2.0$, where the system is clearly an isotro-

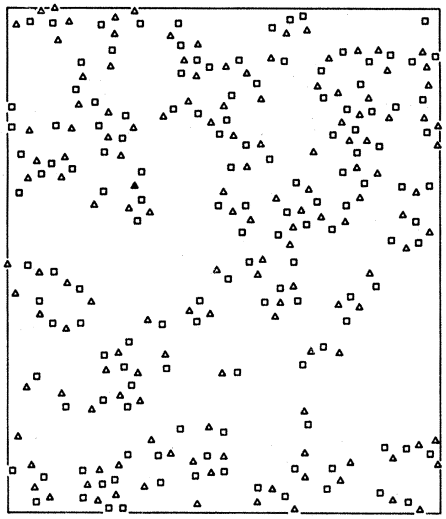

FIG. 9. Distribution of disclinations for $T^* = 1.11$, $\rho^* = 0.888$. This temperature is 5% above the melting temperature and is in the intermediate region. The density of disclinations is now so great that we cannot tell whether they all form bound $(+-)$ pairs. Note also that they are inhomogeneously distributed.

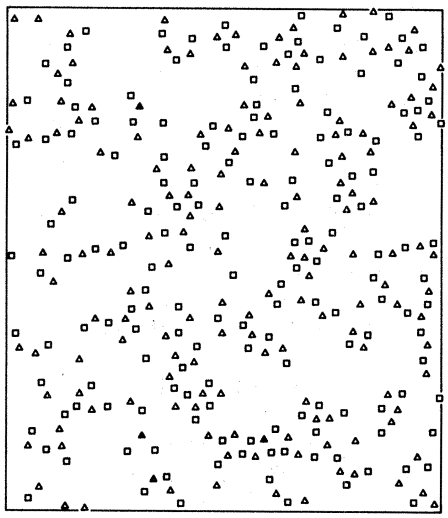

FIG. 11. Distribution of disclinations at $T^* = 2.0$ and $\rho^* = 0.888$. At this density and temperature the system appears to have all the properties of a hot dense fluid. The disclinations are very dense at this temperature and there appears to be some free disclinations.

pic liquid, the disclinations appear as in Fig. 11. Here the density of defects is so great that it is difficult to determine whether or not they are free.

We now estimate the core energy E_c for the dislocations near melting. We can determine the value for E_c by computing the density of defects n in units of disclinations per particle. The density n should be a function of temperature given by

$$n \sim \exp(-\mu/k_B T) \ ,$$

where μ is the activation energy for an excitation. From our plots of the defects we see that the basic excitation consists of a pair of bound dislocations or equivalently a quadruple of disclinations. Then, neglecting any core interaction energy, E_c for a single dislocation will be $\mu/2$. We determined N by counting the number of defects for a number of configurations. Plots of $\ln(n)$ vs $1/T^*$ are shown in Fig. 12.

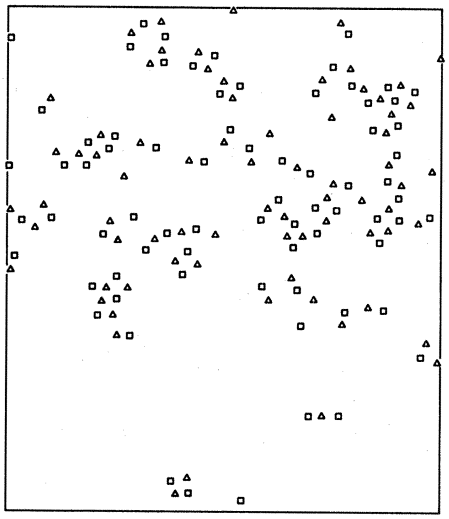

FIG. 10. Distribution of disclinations at $T^* = 1.11$ and $\rho^* = 0.888$. By comparing the figure with Fig. 8, we see that the number of dislocations and disclinations fluctuates from configuration to configuration. The notation is the same as in Fig. 8.

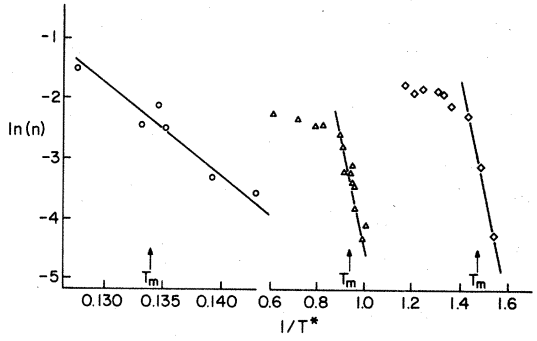

FIG. 12. Logarithm of the number of disclinations per particle as a function of $1/T^*$. The straight lines are least-square fits to the points at lower temperatures. In the text we showed how the slope of these lines could be used to determine the energy of a dislocation: ○ for $\rho^* = 1.143$, Δ for $\rho^* = 0.888$, ◇ for $\rho^* = 0.856$.

At $\rho^* = 0.856$, $E_c \sim 14T_m^*$ and at $\rho^* = 0.888$, $E_c^* = 9T_m^*$. We find that just at melting there are about 50 disclinations for 1024 particles.

However, we should note that the dislocation pairs are not uniformly distributed. There is a very strong tendency to cluster. It is clear that the density of dislocation pairs is so high in some regions that they cannot be treated as a homogeneous dilute gas of excitations. The basic application of the HN theory may not be valid just above T_m. A very similar situation holds for the planar magnet.[14]

The first-order interpretation of melting makes no predictions regarding the presence of topological defects. However, just above melting, it is plausible that some free dislocations will appear. The liquid part of a two-phase region would be expected to show many such defects, the solid part very few. This is consistent with our plots of defects.

At the present stage of our analysis of the topological defects we cannot make any distinction between a first-order transition and KT transition. Nor can we make any distinction between a hexatic phase and a two-phase region.

G. Particle trajectories

We have plotted the Monte Carlo (MC) trajectories of the particles in our system for several runs of different duration. Each plot contains the positions of each particle, usually plotted at 10 times, separated by consecutive runs of equal duration. The positions for each particle are connected by straight lines. From such pictures we may gain some insight into the nature of each of the phases discussed so far.

In the solid region, at all densities and temperatures, the particles are clearly well localized on their lattice sites. In the solid just below melting one can see some evidence for diffusive motion. For example, at $T^* = 1.05$, $\rho^* = 0.888$, which is 1% below melting, we see the pattern shown in Fig. 13. This figure contains the particle trajectories for about 18 000 MC passes and contains 10 points separated by 1800 passes.

In the liquid phase, the particle trajectories look completely disordered for runs of a few thousand passes. However, even at $T^* = 3.0$ for a run of 200 passes, short-range order is quite apparent, as seen in Fig. 14. Here we see well-ordered patches with about 10–20 particles each. The patches are randomly oriented and separated from each other by disordered boundaries. This order may be responsible for the large peaks in $S(k)$ and increased structure in $g(r)$ found in dense 2D liquid systems.[3,8,9]

In the intermediate region we find results such as those shown in Figs. 15 and 16 which contain the particle trajectories of two succesive MC runs of 5 000 passes at $T^* = 1.11$ and $\rho^* = 0.888$. As one can

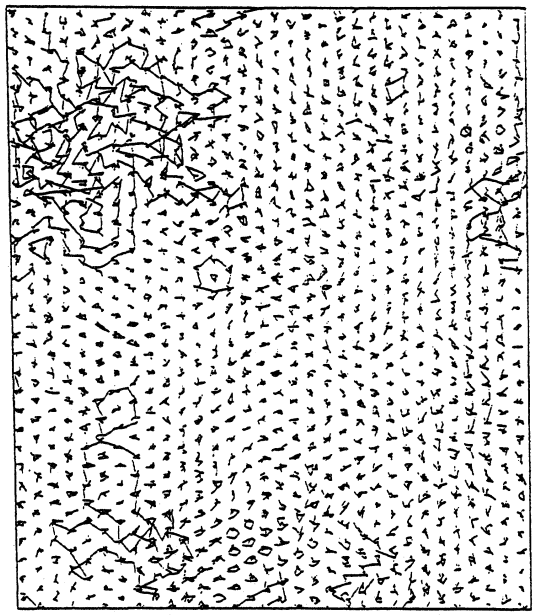

FIG. 13. Monte Carlo (MC) trajectories at $T^* = 1.05$ and $\rho^* = 0.888$. Ten points, separated by 1800 passes, are plotted for each particle. The total number of passes is 18 000. This temperature is just below melting. The solid appears to be well ordered with regions of "diffusion."

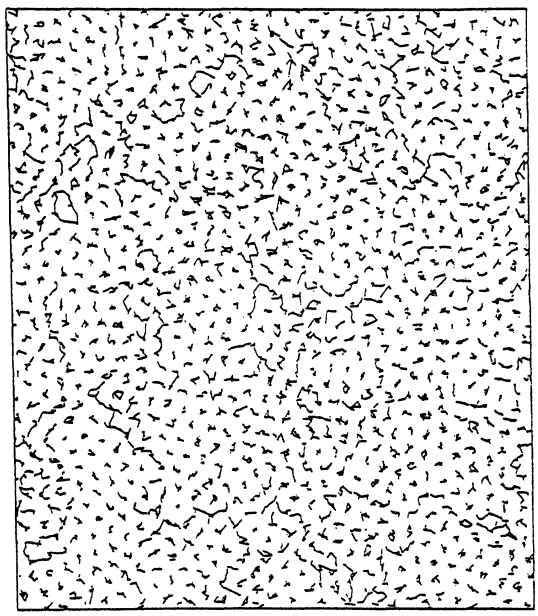

FIG. 14. MC trajectories for $T^* = 3.0$, $\rho^* = 0.888$. Ten points for each particle separated by 20 passes. Total passes 200. In the hot disordered fluid order is present on short MC "time scales."

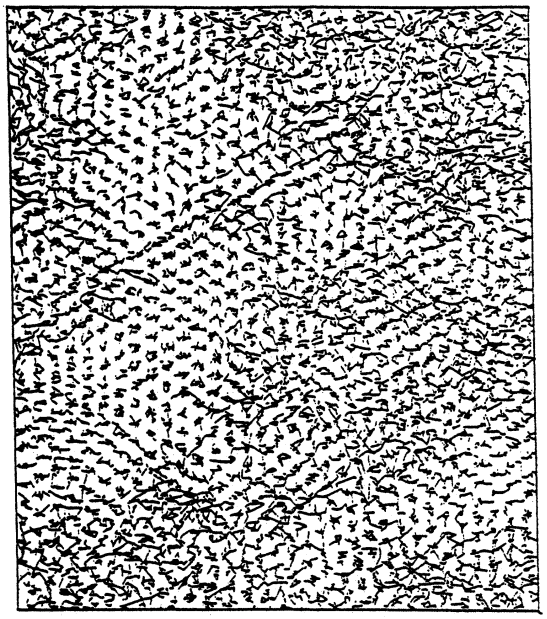

FIG. 15. MC trajectories for $T^* = 1.11$, $\rho^* = 0.888$. Twenty points per particle, 250 passes between the points. Total of 5000 passes.

see, there are two types of regions, solid-like and liquid-like. Also, we can see that the solid-like region appears to be growing between Figs. 15 and 16. Thus there is evidence that the size and shape of the ordered region is not fixed over time. If one looks at a trajectory picture for 50 000 passes, the system looks disordered, implying that the boundaries of the ordered regions have moved over large distances. On a time scale of 200 passes, we obtain the picture shown in Fig. 17. Here the region which looks disordered over 5000 passes is on a short time scale much more ordered with perhaps a few patches of order oriented in different directions from the large ordered region.

For the same density we show pictures at $T^* = 1.22$ and 1.28 for 2000 passes (Figs. 18 and 19). These temperatures are above and below T_2, the upper boundary of the intermediate region. We note that at $T^* = 1.22$ there still is a large ordered region, whereas at $T^* = 1.28$ there appears to be much smaller patches of order. In Fig. 20, at $T^* = 1.075$, 1% above melting, the disordered region takes up a sizable fraction of the total area.

The interpretation of these pictures is difficult. They could be interpreted in terms of two-phase coexistence as was done by Toxvaerd.[23] In this case we would expect that the fraction of ordered region would decrease with temperature. This is certainly true if we look only at pictures made from 5000 MC passes. However, if we decrease the duration over which we look at the trajectories then we find only small changes in the fraction of solid present. For example, compare Fig. 15 at $T^* = 1.11$ with Fig. 18 at $T^* = 1.22$. In a first-order interpretation we do not expect the fraction of solid to change as much as it appears to do at $T^* = 1.11$.

If the intermediate region is hexatic then the or-

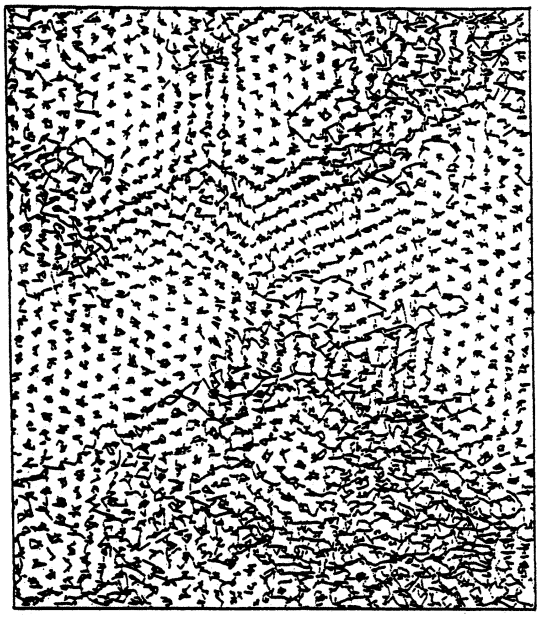

FIG. 16. MC trajectories for $T^* = 1.11$, $\rho^* = 0.888$. This figure is plotted in the same way as Fig. 15, but the initial configuration was taken 5000 passes after Fig. 15.

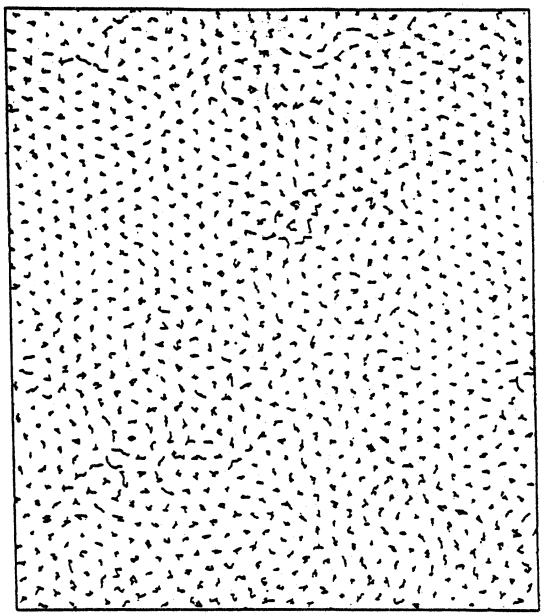

FIG. 17. MC trajectories for $T^* = 1.11$, $\rho^* = 0.888$. Ten points per particle, 20 passes between the points. Total of 200 passes. On this very short time scale the system is comparatively well ordered.

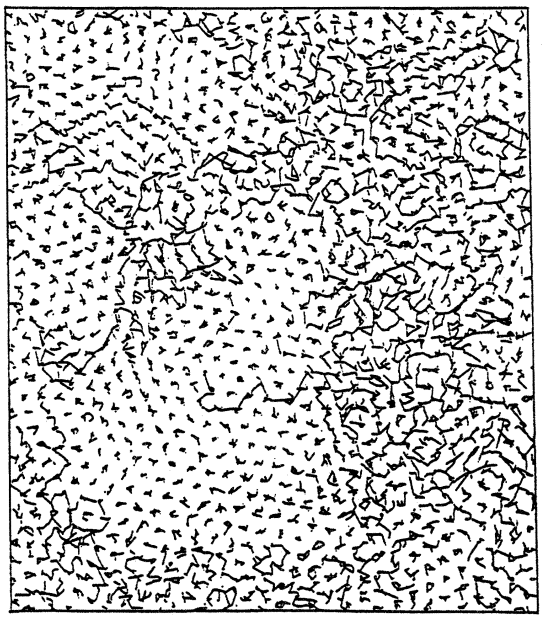

FIG. 18. MC trajectories for $T^* = 1.22$, $\rho^* = 0.888$. Ten points per particle, 200 passes between the points. Total number of passes, 2000. At the higher temperature, in the intermediate region, there are still large "ordered" regions.

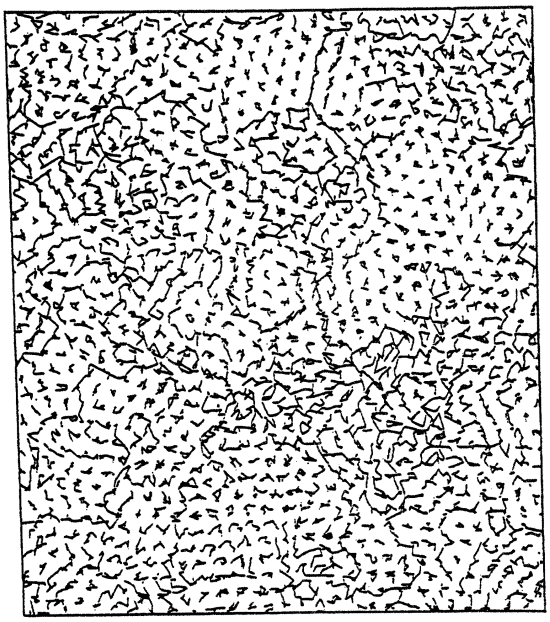

FIG. 19. Same MC trajectories as in Fig. 18 but computed at $T^* = 1.28$, $\rho^* = 0.888$. At this temperature the angular corrrelations clearly decay to zero and we have little order in the system.

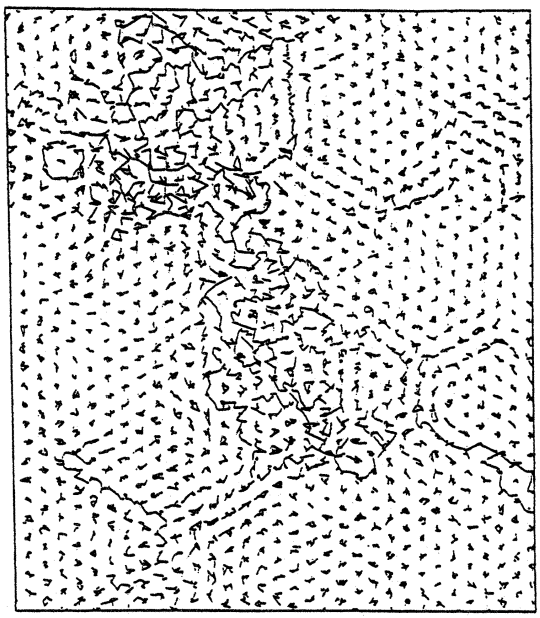

FIG. 20. MC trajectories at $T^* = 1.075$, $\rho^* = 0.888$. Ten points per particle separated by 500 passes. Total number of passes, 5000. This temperature is very near melting and we have considerable order in the system with patches of disorder and some diffusive motion.

dered regions could represent critical fluctuations, since the hexatic phase is a critical region. One must remember that the total real time of our longest runs is equivalent to less than 10^{-8} sec. In a critical region we expect regions of all sizes, the largest of which would last for very long times. We would also expect large ordered regions at all temperatures within a hexatic phase, which we do indeed see if we look at MC runs of different durations.

H. Bond angle configurations

We can construct a representation of a hexatic phase that allows interesting comparisons with spin configurations in the magnetic planar model. In Fig. 21 we show the position and orientation of the vectors representing each bond in a single configuration at $T^* = 1.11$ and $\rho^* = 0.888$. The angle each vector makes with the x axis is six times the angle determined by the Voronoi polygon construction which we used previously to determine the disclinicity at each particle. As can be seen, there is a general trend for the vectors to point in one direction. Also, there is no evidence of two phases, one well ordered and the other disordered.

To make a comparison with the planar model, we

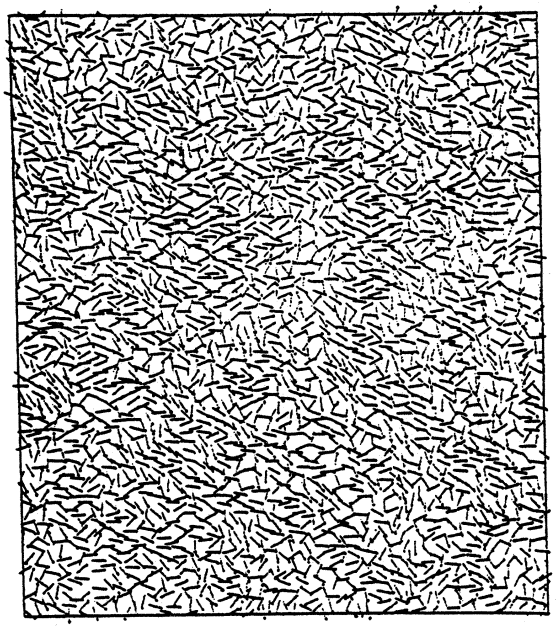

FIG. 21. Bond angle field for one configuration at $T^* = 1.11$, $\rho^* = 0.888$. There is a tendency for the bond angle vectors to point to the right.

have constructed Fig. 22. This represents the same bond angle field in Fig. 21, except that we have averaged over small square regions $\sigma \times \sigma$ in size. We then rescaled to unit vectors and placed the resulting vectors on a square lattice. In Fig. 23 we show the spin configuration for the planar model about 10%

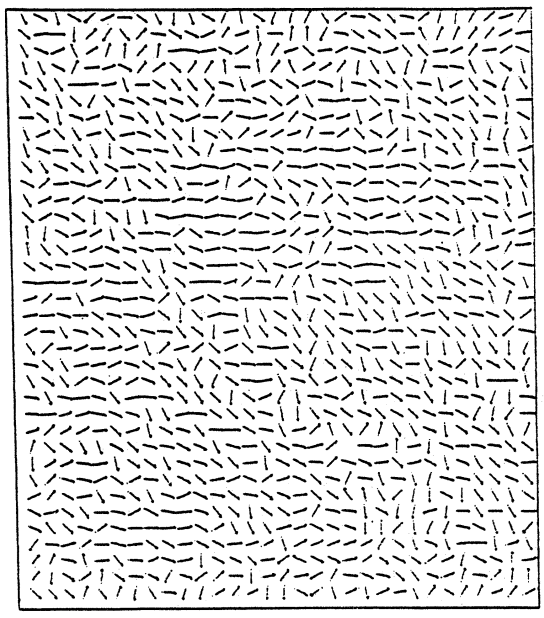

FIG. 22. Bond angle field in Fig. 21 was spatially averaged over a region $\sigma \times \sigma$, and the average bond angle vector was then normalized to unity. Again we see a general alignment to the right.

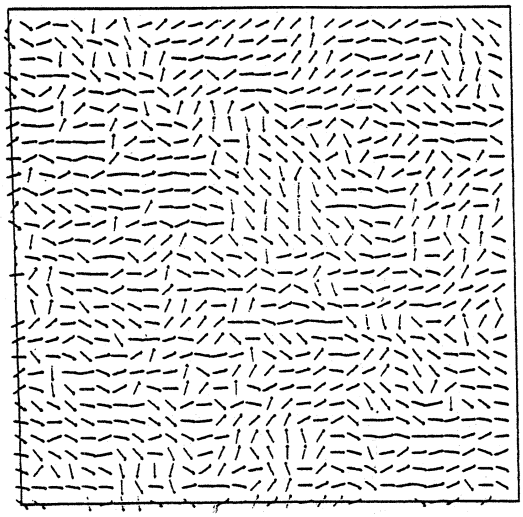

FIG. 23. Typical spin configuration for the planar magnetic model at $T^* = 0.82 (T_c^* = 0.89)$. This figure is presented for comparison with Fig. 22. It was made at a temperature a little below the transition temperature where the system shows power-law decay for the spin correlations.

below T_c generated by molecular dynamics simulations. Figures 22 and 23 look very similar. This is consistent with a hexatic phase interpretation of the intermediate region. The bond angle field for a solid just below the melting temperature also looks similar to Figs. 21 and 22 since there is little difference between weakly decaying orientational correlations and long-range correlations in a finite system.

III. HIGH-DENSITY LENNARD-JONES SYSTEM

We have also carried out a series of simulations on the Lennard-Jones system at a reduced density $\rho^* = 1.143$. This study was carried out for two reasons. First, HN have suggested that the character of the melting transition might change as one moves along the melting curve from low to high densities. In the Introduction we pointed out that there may be an "upper" triple point above which the presumed hexatic phase no longer exists. This is shown in Fig. 1(a). Second, at this much higher density the repulsive part of the potential tends to dominate in potential energy calculations. It thus tends to determine the configurations that are important in the system. In effect we are, at this density, studying a system with a rather different interaction potential. Our results are as follows.

In the solid phase the behavior of the energy, pressure, and orientational order are very similar to the behavior on the two low-density isochores. We can again establish a melting temperature; the elastic constant K again abruptly drops to zero from a relatively large finite value. This drop occurs at $T^* = 7.45$.

However, K cannot be fitted by the universal form suggested by the HN theory, and the discontinuity is now larger than 16π. This is shown in Fig. 6. At this transition the behavior of both E^* and P^* is quantitatively different from that found earlier. Both these quantities show a very sharp rise—much sharper than before. In addition, this is followed by a second sharp increase in slope at $T^*=8.50$. This is shown in Fig. 2. Thus the energy and pressure now clearly show that there is an intermediate region between $T^*=7.65$ and $T^*=8.50$. At the lower densities the behavior of the energy and pressure could also be interpreted in the same way. However, the width of the region, as a fraction of T_m^* was narrower and the second anomaly was very much weaker.

The long-range orientational order of the solid disappears abruptly at the melting temperature, confirming our preliminary determination of that point. In the intermediate region, $g_6(r)$ decays exponentially up to $r\sim 6-10$. For larger r, a slow decay appears to set in and the function oscillates about zero with values ranging from $+0.06$ to -0.06. This behavior is very different from that found on the low-density isochores. At this higher density, decay is much faster and asymptotically the value is close to zero.

The qualitative behavior of the defects is similar to that found at lower temperatures. However, there is a quantitative change in the density of dislocations at T_m^*. It is a factor of 2 larger in the high-density system. We computed the core energy from the data shown in Fig. 11. We find that $E_c\sim 11k_BT$. This value is not very different from the low-temperature values quoted in Sec. II F.

At this density we see no evidence to support the KT theory of melting. The elastic constant K does not show the expected behavior and the orientational order shows little evidence for a hexatic phase. The data we have generated from our simulations is consistent with a first-order melting transition.

Our analysis of the topological defects are not sufficiently detailed to allow us to draw any conclusions. Dislocations are numerous at T_m^*. They may play an important role in the melting transition. However, the density of dislocations is sufficiently great that we are not really able to say anything about whether they are unbound or whether the disclinations are unbinding at T_m^*. HN have suggested that a "premature" unbinding of disclination pairs would lead to a first-order transition.

The behavior of the high-density Lennard-Jones system allows us, with the minimum of assumptions, to predict the melting behavior of both the inverse 12th power potential and the hard-disc system. If we assume that the qaulitative features of the high-density transition will be maintained as we increase the density, then we can conclude that the inverse 12th power potential will lead to the same behavior. This is because, at sufficiently high densities, the Lennard-Jones system will be dominated entirely by the repulsive part of the potential. A system interacting via an inverse 12th power potential is characterized by a single thermodynamic variable $\Gamma_{12}=\epsilon/k_BT$ (σ/a_0).[12] Here ϵ is the Lennard-Jones strength parameter, σ the length parameter, and a_0 the mean particle spacing. Thus when its properties have been established at one point (T,A) on the melting curve, they are known at all other points; the melting curve is given by $\Gamma_{12}=$const. We therefore believe that this system will show a first-order melting transition and will not have a hexatic phase.

The hard-disc system should be qualitatively well described by the inverse 12th power system. It is therefore expected to show a first-order transition and no hexatic phase. We shall see in Sec. IV that this prediction appears to be born out by our simulations.

IV. HARD-DISC SYSTEM

The hard-disc system was one of the first systems to be studied by molecular dynamics and Monte Carlo methods.[8] Over a fairly large period of time a considerable amount of data has been collected on it. In particular the melting transition has been studied carefully. It is believed to be a first-order transition with a freezing density $\rho_r=\rho/\rho_0=0.7611$ and a melting density $\rho_r=0.798$. Here ρ_0 is the close-packed density.[30] In Sec. III we gave a plausible argument that the melting transition in this system would be very similar to that in the high-density Lennard-Jones system. Since our data on the high-density Lennard-Jones system are consistent with a first-order transition, we expect that our simulations will confirm the earlier work on the transition.

Our simulations were done on a 1024 hard-disc system and most of our runs were made near the melting and freezing transitions. We computed $S(k)$, $\langle u^2\rangle$, $g_6(r)$, and the disclination density. We also made plots of the disclination configurations and the Monte Carlo trajectories. Our results are as follows.

We find that if we start in the solid phase and decrease the density, then $\langle u^2\rangle$ suddenly increases at $\rho_r=0.781$ and $S(k)$ drops abruptly at $\rho_r=0.775$. Both these densities are lower by 2–3% than the accepted melting density.

The disclination density rises from $n=0.05$ at $\rho_r=0.781$ to $n\sim 0.15$ at $\rho_r=0.775$. This increase is greater than we observed in the low-density Lennard-Jones system and suggests that the transition may be controlled more by the number of defects than their unbinding. Although we also have some evidence that at melting there are some free disclinations. At densities well inside the solid phase the defects appear only as bound pairs of dislocations. It is worth pointing out that in this system configura-

tions only differ in "entropy" content. Hence the binding of dislocations has to be explained on purely entropic grounds.

The angular correlation function $g_6(r)$ shows long-range order for all densities above $\rho_r = 0.781$. Between $\rho_r = 0.781$ and $\rho_r = 0.763$, $g_6(r)$ shows a slow decay across the system. Below $\rho_r = 0.763$ the function shows exponential decay. There is thus an intermediate region between these densities. The width $\Delta\rho_r = 0.018$ is about one-half of that found in the earlier studies of the hard-disc transition where $\Delta\rho_r = 0.037$. However, we note that the lower density at which the intermediate region ends $\rho_r = 0.763$, is very close to the freezing density $\rho_r = 0.761$, found in the earlier work. The discrepancy is almost entirely confined to the melting density.

In the intermediate region, the particle trajectory plots show the same behavior as those of the Lennard-Jones system. There is some evidence that the boundaries of the ordered regions do not change as fast as in the Lennard-Jones system. In the intermediate region there are free dislocations and, in addition, there are some free disclinations. A typical plot of the defects is shown in Fig. 24 for $\rho_r = 0.775$. The presence of free disclinations just above the melting density suggests that they may have become unbound just before melting, in which the transition would be expected to be first order.

The data we have generated on the hard-disc system are consistent with it being a first-order transition. While our freezing density is very close to the currently accepted value, our melting density differs from the earlier values by 2–3%.

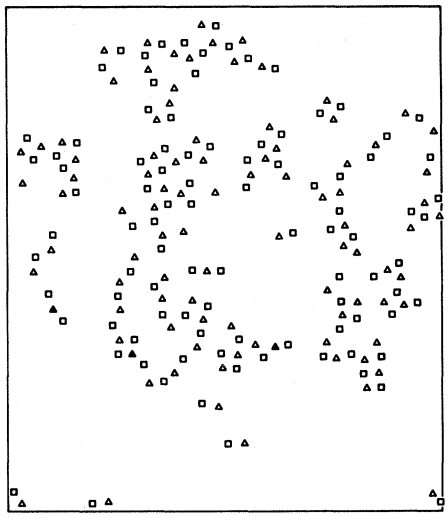

FIG. 24. Distribution of disclinations in the hard-disc system at the reduced density $\rho_r = 0.775$.

V. CONCLUSIONS

In the main text of this paper we have summarized our results for each system which we simulated. We start this section by giving our overall summary of our findings. We then turn to a discussion of the basic difficulties in simulation studies of this type. Finally, we suggest areas where future work might yield interesting results.

We feel that our results for both the high-density Lennard-Jones and the hard-disc systems are consistent with a first-order transition. An alternative statement would be that there is no feature of these transitions that suggests that they are driven by the unbinding of topological defect pairs. Since the Kosterlitz and Thouless transition is not expected to be universally valid in all two-dimensional systems, we should not be surprised that first-order transitions can be found in two dimensions. More careful and extensive simulations on the hard-disc system might show whether there is a real discrepancy between the older estimates of the melting density and those found by our methods. It would also be interesting to study the behavior of the dislocation pairs in this system. One would like to understand why they appear only as bound pairs in a purely entropic system.

We next turn to the low-density Lennard-Jones system. We believe that our simulation results do not lead us to a definite conclusion as to the nature of the melting transition or to whether or not a hexatic phase exists. The single set of data that unambiguously suggests that the melting transition is of the Kosterlitz and Thouless type is the behavior of the elastic constant K. In Sec. II we displayed our data and showed that its temperature dependence was very close to that predicted by the HN theory. In addition, the discontinuity in K was also very close to the theoretical prediction of 16π.

We remind our readers that both these statements are true for both low-density isotherms. Morf[7] found the same behavior in the one-component plasma. It is also worthwhile recalling that our simulations showed that we had a unique melting point: $\langle u^2 \rangle$ increased dramatically at T_m, the peaks in $S(k)$ dropped dramatically, and the angular correlation function changed its asymptotic behavior at that temperature. The melting temperatures, as we estimate them, on these two isotherms are lower than those given by Toxvaerd. There is clearly a need for further work to try to reconcile these different estimates. Since we have no other strong evidence that the system is behaving as the theory predicts, one is tempted to try to explain away the behavior of K. It has been suggested that what we are seeing is the "melting" of a metastable solid. That is to say we have in our simulations superheated the solid above its true melting point which, when it becomes sufficiently unstable, melts via the Kosterlitz-Thouless mechanism.

This leads to results that agree with the predicted behavior for K. While we cannot produce an argument which completely disposes of this suggestion, we find it at least somewhat implausible that at two different densities a metastable solid melts in accordance with the predictions of equilibrium statistical mechanisms. Moreover, we have some evidence from our simulations that we may be able to cool into the so-called metastable region. When we cool into the solid just below melting we find reasonably well ordered crystal configurations with small values of $\langle u^2 \rangle$. Moreover, in medium length Monte Carlo runs the asymptotic value of the angular correlations does not reach the same value as it had when the system was heated to the same temperature. We will investigate whether this result can be changed by larger runs. If we can "reconstruct" the solid by cooling, we feel this would be strong evidence against the idea that our melting transition is that of a metastable solid. We also believe it is worthwhile to carry out some careful simulations to determine over what range of melting densities K shows the predicted behavior. It is especially important to try to determine whether the temperature dependence of K is the same on cooling as on heating.

We now turn to a discussion of the intermediate region we found in our simulations. All our data in this region can be interpreted as evidence either for it being a two-phase region or a hexatic phase. We see nothing conclusive in our data. A basic difficulty in this region is that we appear to be dealing with a system which contains very long relaxation times. This fact in itself could be explained in either the two-phase hypothesis or hexatic phase hypothesis. The hexatic phase in the HN theory is a critical region with correspondingly long relaxation times. On the other hand, in a two-phase region we expect slow changes in time as the two phases change their boundaries and reform. Our current estimates are that we need to run simulations at least ten times longer than our longest runs to obtain better estimates of the relaxation times and perhaps obtain reasonably accurate equilibrium values for the angular correlation function and structure function. We do, however, think it worthwhile to try to compute the value of the Frank constant in the region. This is predicted to have a discontinuity at the upper transition point T_2^* of $72/\pi$. We have done some work on this quantity and have found values of approximately this magnitude. Our data are very preliminary and we need to do much more work.

A rather different simulation has been suggested. The idea is to prepare a hexatic phase in the appropriate region of the density temperature plane and then examine whether it is a stable phase. The phase can presumably be readily prepared by applying a field which will bring about angular order without producing crystalline order. The field can then be removed and a long Monte Carlo run conducted to see whether the system behaves as predicted by the theory. This kind of simulation seems to us to be worthwhile because it can be argued that our inability to find the hexatic phase is due to the fact that on either heating or cooling we rather suddenly pass through a phase boundary with the consequence that a homogeneous hexatic phase does not form. A series of domainlike structures may form which will obscure the true nature of the phase. The external field which we apply may enable us to eliminate these domains and produce a homogeneous phase which might then be stable over long periods of time. We have begun some preliminary experiments of this kind.

We conclude by discussing two questions. Our simulations are of necessity performed on finite systems. One must, therefore, ask whether the finite size of our system is significantly affecting the nature of the melting phenomenon. We have two comments to make on this question. First, we see in our simulations direct evidence for the lack of any long-range positional order which is characteristic of the behavior of 2D systems. The peaks in the structure factor in the solid phase behave as theory predicts and are distinctly different from those in a 3D solid. In addition, it is well established that in simulations on systems of the same size as ours, $\langle u^2 \rangle$ will show the characteristic $\ln(N)$ dependence in accord with theory. Thus even small 2D systems show the expected "large system" behavior. Our second point is that it is conceivable that the weak order characteristic of 2D systems could in some more subtle way be altered in a small system, and thus the nature of the transition could be changed. While this argument has some appeal, we do not find it very convincing. This is because the simulated transition in the planar magnetic model seems to be in good quantitative agreement with theory. We then have to understand

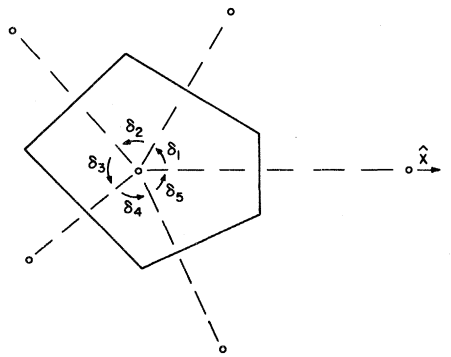

FIG. 25. Solid lines represent the boundary of the Voronoi polygon. The angles formed by the dashed lines and the x axis are the bond angles. The angles $\{\delta_i\}$ are used in the proof.

why the finite size has no appreciable effects in that system but are able to completely alter the nature of the transition in the 2D solid-fluid system.

Our final question has to do with the "time scales" of our simulations. These are indeed quite short, perhaps no longer than 10^{-8} sec in our long runs. A Debye time is about 10^{-11} sec, so we are working on time scales of about 1000 Debye times. Another comparison is that 10^{-8} sec is about ten times longer than the transit time of a sound wave across our system. Since the expected hexatic phase is a critical region, we must expect it to be dominated by very long time scales. These two facts suggest that it may be exceedingly difficult to simulate equilibrium conditions in a hexatic region. We have not at the moment found a way to explore this problem further.

ACKNOWLEDGMENTS

The authors acknowledge useful conversations with David Nelson and John Weeks. This work has been supported by the NSF through the Cornell Materials Science Center under Grant No. DMR-76-81083.

APPENDIX: NEAREST NEIGHBORS, VORONOI POLYGONS, AND DISCLINATIONS

In this Appendix, we define the nearest neighbors in terms of the Voronoi polygons and show that a disclination is located at a particle which has a coordination number z, not equal to six.

A Voronoi polygon is defined as the boundary of a region enclosing a particle i, such that every point within that region is closer to particle i than any other particle. The sides of the Voronoi polygon are the perpendicular bisectors of the lines joining particle i with z other particles which we define as the nearest neighbors of particle i, as shown in Fig. 25. We now show that a particle with z nearest neighbors is a disclination of strength $m=6-z$. At a disclination of strength m, the bond angle turns by $m\pi/3$ in transversing the circuit containing the bonds associated with that particle.

To prove this result we convert the bond angles into a set of angles $\{\beta_i\}$ with values between $-\pi$ and π such that a total change in the bond angles of $m\pi/3$ corresponds to a change in the β_i of $2\pi m$. We define the angles δ_i as shown in Fig. 25. Clearly

$$\sum_{i=1}^{z}\delta_i=2\pi \ . \tag{A1}$$

We now define the β_i:

$$\beta_i=\left[6\sum_{j=1}^{i}\delta_i\right]\mathrm{mod}2\pi, \quad -\pi\leq\beta_i\leq\pi \ . \tag{A2}$$

The factor of 6 is used to convert the problem from one where, if $\Delta\delta_i=m\pi/3$, then $\Delta\beta_i=2\pi m$. We also define the angles

$$\alpha_i=\delta_i-2\pi/z \ . \tag{A3}$$

Then we have, using Eq. (A1):

$$\sum_{i=1}^{z}\alpha_i=0 \ . \tag{A4}$$

The β_i are now given by

$$\beta_1=\left[6\alpha_1+\frac{12}{z}\pi\right]\mathrm{mod}2\pi=6\alpha_1+\left[\frac{12-2z}{z}\right]\pi$$

$$=6\alpha_1+\frac{2m\pi}{z} \ , \tag{A5}$$

$$\beta_{i+1}=\beta_i+\frac{2\pi m}{z}+6\alpha_{i+1} \ ,$$

where by definition from (A2), $-\pi\leq 6\alpha_{i+1}+2\pi m/z\leq\pi$. Now the change in β_i from one angle to the next is

$$\Delta\beta_i=\beta_{i+1}-\beta_i=6\alpha_{i+1}+\frac{2\pi m}{z} \ , \tag{A6}$$

where $\beta_{z+1}\equiv\beta_1$ and $\alpha_{z+1}\equiv\alpha_1$. We sum up the $\Delta\beta_i$ and obtain

$$\sum_{i=1}^{z}\Delta\beta_i=6\sum_{i=1}^{z}\alpha_{i+1}+2\pi m=2\pi m \ . \tag{A7}$$

The last step follows from Eq. (A4). This completes the proof. A disclination of strength $m=6-z$ is located at a particle with z neighbors.

---

*Present address: Department of Physics, Rutgers University, Piscataway, N.J. 08854

[1]N. D. Mermin, Phys. Rev. 158, 383 (1967).
[2]D. A. Young and B. J. Alder, J. Chem. Phys. 60, 1254 (1974).
[3]R. C. Gann, S. Chakravarty, and G. V. Chester, Phys. Rev. B 20, 326 (1979).
[4]R. E. Peierls, Helv. Phys. Acta 7, 81 (1934); Ann. Inst. Henri Poincaré 5, 177 (1935).
[5]L. D. Landau, in *Collected Papers of Landau,* 2nd printing, edited by D. Ter Haar (Pergamon, London, 1967), p. 193.
[6]B. Jancovici, Phys. Rev. Lett. 19, 20 (1967); H. J. Mikeska and H. Schmidt, J. Low Temp. Phys. 2, 371 (1970), Y. Imry and L. Gunther, Phys. Rev. B 3, 3939 (1971).
[7]R. H. Morf, Phys. Rev. Lett. 43, 931 (1979).
[8]W. W. Wood, in *Physics of Simple Liquids,* edited by H. N. Temperley, J. S. Rowlinson, and G. S. Rushbrooke (Elsevier/North-Holland, Amsterdam, 1968).

[9]F. Tsien and J. P. Valleau, Mol. Phys. 27, 177 (1974); S. Toxvaerd, J. Chem. Phys. 69, 4750 (1978); P. L. Fehder, *ibid.* 52, 791 (1970).
[10]B. J. Alder and T. E. Wainwright, Phys. Rev. 127, 359 (1962).
[11]J. M. Kosterlitz and D. J. Thouless, J. Phys. C 6, 1181 (1973).
[12]J. M. Kosterlitz and D. J. Thouless, Prog. Low Temp. Phys. 7, 373 (1978).
[13]W. L. McMillan (unpublished).
[14]J. Tobochnik and G. V. Chester, Phys. Rev. B 20, 3761 (1979).
[15]D. R. Nelson and J. M. Kosterlitz, Phys. Rev. Lett. 39, 1201 (1977).
[16]V. Ambegaokar, B. I. Halperin, D. R. Nelson, and E. D. Siggia, Phys. Rev. B 21, 1806 (1980).
[17]V. Ambegaokar, B. I. Halperin, D. R. Nelson, and E. D. Siggia, Phys. Rev. Lett. 40, 783 (1978).
[18]A. M. Berker and D. R. Nelson, Phys. Rev. B 19, 2488 (1979).
[19]A. P. Young, Phys. Rev. B 19, 1855 (1979).
[20]L. D. Landau and E. M. Lifshitz, *Course of Theoretical Physics, Elasticity Theory* (Addison-Wesley, Reading, 1970), Vol. 7.
[21]P. G. De Gennes, *The Physics of Liquid Crystals* (Oxford University, New York, 1974).
[22]F. F. Abraham, Phys. Rev. Lett. 44, 463 (1980).
[23]S. Toxvaerd, Phys. Rev. Lett. 44, 1002 (1980).
[24]B. I. Halperin and D. R. Nelson, Phys. Rev. Lett. 41, 121 (1978); 41, 519(E) (1978); Phys. Rev. B 19, 2457 (1979).
[25]D. Frenkel and J. P. McTague, Phys. Rev. Lett. 42, 1632 (1979).
[26]H. S. M. Coxeter, *Introduction to Geometry,* 2nd ed. (Wiley, New York, 1961); G. L. Dirichlet, Journal für die reine und angewandte Mathematik 40, 209 (1950).
[27]S. Toxvaerd, J. Chem. Phys. 69, 4750 (1978).
[28]D. R. Squire, A. C. Holt, and W. G. Hoover, Physica (Utrecht) 42, 388 (1968). At finite pressure $\lambda = C_{12} + P$ and $\mu = C_{44} - P$. See G. A. Stewart, Phys. Rev. A 10, 671 (1974).
[29]The fitting procedure consisted of computing the least-squares best value for ν and c at various temperatures T_m^*. The temperature with the minimum standard deviation in the data from the fitted curve was chosen as T_m^*.
[30]J. L. Tallen, Phys. Rev. B 22, 453 (1980).
[31]J. P. McTague, D. Frenkel, and M. P. Allen, in *Ordering in Two Dimensions,* edited by S. K. Sinha (North-Holland, New York, 1980).